

Synthesis and characterization silica-MB@GO-NH₂ particle as fluorescence-based chlorine sensor

Fadhil R. A. A. Fatah¹, Isnaini Rahmawati¹, Jarnuzi Gunlazuardi¹, and Afiten R. Sanjaya^{1*}

¹ Department of Chemistry, Mathematics and Natural Sciences, Universitas Indonesia; Kampus UI Depok, 16424, Indonesia

* Correspondence: afiten.rahmin@sci.ui.ac.id

Accepted Date: December 31, 2023

Cite This Article:

Fatah, F. R. A. A., Rahmawati, I., Gunlazuardi, J., & Sanjaya, A. R. (2023). Synthesis and characterization silica-MB@GO-NH₂ particle as fluorescence-based chlorine sensor. *Environmental and Materials*, 1(2), 96-109. <https://doi.org/10.61511/eam.v1i2.2023.399>



Copyright: © 2023 by the authors.

Submitted for possible open access article distributed under the terms and conditions of the Creative Commons Attribution (CC BY) license (<https://creativecommons.org/licenses/by/4.0/>)

Abstract

In this research, we developed a fluorescence-based sensor to determine the sodium hypochlorite concentration (NaOCl) in tap water and swimming pool water samples. The detection of NaOCl was conducted by measuring the luminescence response of analyte in the paper-based sensor modified Silica-MB@GO-NH₂ material were synthesized using Hummer's and Stober's methods under UV Light irradiation. Additionally, the prepared material exposed a couple peak 2D and 2G at 2938 cm⁻¹ and 3286 cm⁻¹ with ID/IG ratio 0.98 using Raman characterization which appropriate with the presence of GO structure in the mixture. This result was validated by the appearance of several functional groups like Si-O-Si, NH, OH, and C-C at 1079, 1391, 1611, and 3457 cm⁻¹, respectively. Moreover, the existence of Si-O-Si bond indicates that the silica-MB interaction was perfectly formed, which plays the main role to absorb ultraviolet light that is used as sensor probe. The morphology of particles depicted an aggregated formation of spherical structure with 288 nm particle size, indicating the existence of silica-coated methylene blue. In this work, the paper-based sensor modified Silica-MB@GO-NH₂ can detect the NaOCl species with concentration range 10-150 μM (R₂ = 0.9757), a detection limit at 2.60 μM and quantification limit at 7.88 μM. Furthermore, this developed sensor has stable measurement with recovery performance 3.65%-6.67% for tap water and 0.05%-0.14% for swimming pool water. This result indicates that the prepared sensor can be potentially applied to calculate the hypochlorite species in the aquatic environment.

Keywords: fluorescence; NaOCl; paper-based sensor; particle; sensor

1. Introduction

Sodium hypochlorite (NaOCl) is an essential oxidizing agent found in aquatic environments, bleach products, and especially in disinfectant products (Sanjaya et al., 2023). The disinfection solution is derived from the reaction between chlorine gas in water, resulting in the production of hypochlorous acid compounds then dissociate into hypochlorite ions. This ion is often used in the process of purifying water and sterilizing bacteria, such as in tap water or swimming pools. As a result, excessive use of sodium hypochlorite in this water treatment can improve microbiological water quality (Böger et al., 2020). When sodium hypochlorite is consumed in high quantities (5 mL/kg in children, 150-200 mL in adults), or at concentrations greater than 6%, serious poisoning results may occur (Chung et al., 2022). Because of this, prior studies involving humans have suggested that water consumption or the use of water from facilities exposed to sodium hypochlorite (free chlorine) could potentially lead to various health issues, including inflammation, nausea, atherosclerosis, and respiratory problems (Chung et al., 2022; Rahmawati et al., 2022a). Briefly, detecting this compound has become crucial, particularly in assessing its selectivity in aquatic environments that require monitoring.

Over the past few decades, numerous analytical methods for determining NaOCl concentration have emerged, including colorimetry (Carlsson et al., 1999), amperometry

(Thiagarajan et al., 2011), and electrochemical method (Endo et al., 2004). These methods often require complex instruments and a professional operator, making it more challenging to investigate NaOCl concentration. Recently, the fluorescent method has become famous as a preferred sensor detection method among researchers. Fluorescence enables the detection of chemical compounds that exhibit fluorescence under UV-A light. This method offers significant advantages, including high sensitivity, minimal reagent usage, rapid process, small sample volume requirements, and accessibility for sample preparation and operation (Bose, Thomas, Kavitha, et al., 2018; Shahzad et al., 2009).

There are a lot of fluorescence probes, such as TAM (Triphenyl Amine-Based) in human body cells (Goswami et al., 2015), Rhodamine B nanospheres with amino groups functionalized graphene oxide (RBDS/GO-NH₂) in aquatic environments (Q. Yang et al., 2019), and Nitrogen-doped carbon quantum dots (N-CQDS) in tap water and swimming pools have been successfully employed for NaOCl sensing and monitoring (C. Yang et al., 2019). However, these materials also have disadvantages, such as a limited control over physicochemical properties, toxicity, and might of inadequate enhancement of photostability in fluorescence instruments (Sharma et al., 2022). Despite these challenges, fluorescence systems require a photon-emitting device on the surface (Enderlein et al., 1999). One advantageous approach is developing paper-based sensors, which are relatively straightforward to create and can be employed for on-site active substance detection (Yao et al., 2022). Analyzing materials with a fluorophore mechanism is crucial to enhance fluorescence intensity and overcoming these limitations.

Therefore, the chosen material must exhibit a broad fluorescence wavelength and photostability to ensure balanced performance during measurements. Methylene blue (MB) serves as a Near Infrared (NIR: 700–900 nm) fluorophore is noted to have extensive use in applications involving chemiluminescence and fluorescence, making it a promising candidate for NaOCl detection (Cwalinski et al., 2020). This was confirmed by previous researchers that the detection of hypochlorite in tap water samples provided an excellent detection limit of 0.1 μ M (X. Huang et al., 2018). Notably, the wavelength of NIR exceeds the other light types, allowing for deeper structural monitoring (Z. Wang et al., 2023). In addition, methylene blue is employed to enhance intensity, enabling easy differentiation between materials or test concentrations (Budner et al., 2022). However, the fluorescence method often encounters self-quenching, a phenomenon in which energy is lost due to collisions between excited and ground-state molecules. This phenomenon can lead to a reduction in fluorescence yield (Baek et al., 2020). To overcome this issue, the measurement process necessitates a material capable of controlling self-quenching, and one such compound is silica.

Silica, also known as silicon (SiO₂), is a mineral compound composed of silicon and oxygen, providing the ability to enhance the photostability of photosensitizer (W. Yang et al., 2004). This is achieved by controlling the aggregate state and preventing the self-quenching effect of MB (Y. Wang et al., 2018). Furthermore, its advantages are the abundant availability, stable fluorescence control results, and ability to maintain fluorescence intensity (Ishmah et al., 2020). As a result, it is perfectly suitable for these measurements. Despite these merits, it is worth noting that silica lacks intrinsic fluorescence intensity and emission properties due to the absence of a fluorophore.

Additionally, silica can interact with MB through hydrogen and electrostatic bonds between the hydroxyl (OH) and alkoxy (OR) groups, forming silica-MB complexes. Nevertheless, silica-MB can only be utilized in conducting tests when paired with a material having a high surface area to enhance sensor performance. Graphene oxide (GO) is an ideal material characterized by a large surface containing carbon sp² and has a rigid structure that allows flexible interactions with foreign substrates (X. Liu et al., 2019). GO manufacturing using the Hummers method offers advantages such as time efficiency, safety, and low toxicity (Smith et al., 2019). This method involves a chemical process that generates graphite oxide by introducing potassium permanganate to a solution containing graphite, sodium nitrate, and sulfuric acid, and it is recognized for its environmental friendliness (J. Liu et al., 2022). However, the experiment may not succeed solely from the presence of GO

since the fluorescence system cannot function correctly due to the quenching mechanism. To resolve this, a substrate capable of oxidizing NaOCl is required. A suitable candidate for this role is the amine functional group (NH_2).

The modified amine structure can induce fluorescence quenching by reacting with NaOCl to form chloramines. This interaction triggers fluorescence blackout through intramolecular charge transfer (ICT), which is the interaction of donor and acceptor electrons, leading to a decrease in fluorescence intensity (Q. Yang et al., 2019). Amine substrate modified onto GO to create GO- NH_2 and enable this interaction. The modification involves hydrogen bonding and electrostatic interaction forming amine-modified GO (GO- NH_2). Subsequently, the combination of silica-MB with GO- NH_2 occurs through hydrogen bonding, obtaining a material known as silica-MB@GO- NH_2 . Furthermore, in fluorescence spectroscopy measurements, significant differences exist between the emission wavelengths of silica-MB@GO- NH_2 and GO- NH_2 , where the GO- NH_2 exhibits distinctive fluorescent color changes that can easily be discerned with the naked eye, allowing for straightforward recognition (C. Yang et al., 2019).

In summary, the fabrication of silica-MB@GO- NH_2 particles was accomplished using the Hummer's and Stober's method. The prepared substrate was developed as paper-based sensor to detect/determine the NaOCl concentration in tap water and swimming pool samples using fluorescence response as probing methods.

The Silica-MB@GO- NH_2 particles have been successfully fabricated for application in paper-based sensors. The substrate is aimed at determining the concentration of NaOCl in tap water and swimming pools, demonstrating good signal response results on the applied fluorescence sensor. Furthermore, the performance test was conducted using the existing probing method, which showed favorable detection limit results for detecting the NaOCl analyte.

2. Methods

2.1. Materials and Instruments

Methylene Blue and NaNO_3 were obtained from WAKO Chemical Industries Ltd, Tetraethyl orthosilicate, poly (vinyl alcohol) (PVA-1788), and 0.45 μm filter paper cellulose nitrate was brought from Merck. Moreover, NaOCl was purchased from Sigma-Aldrich. Scanning Electron Microscopy (SEM) (Jeol JSM-IT200) was used to study the size and morphology of the particle. Raman spectroscopy (HORIBA-TheLabRAM HR Evolution) was performed to investigate crystallinity and molecule interaction. Fourier Transform InfraRed (FTIR) (Shimadzu IR Prestige 21) was employed to determine chemical bonds in the molecule. Ultraviolet Diffraction Reflectance Spectroscopy (UV-DRS) (Shimadzu UV-2450) was used to investigate %reflectance and bandgap on material prior to determining the NaOCl concentration in the sample and UV-A lamp (GEN STAR) used to gain color luminescence was recorded below.

2.2. Synthesis of Silica-MB

The preparation of the methylene blue system covered with silica was carried out based on the Stober method (Greasley et al., 2016). Mix 92 mL ethanol, 17.2 mL H_2O , and 2.48 mL $\text{NH}_3\cdot\text{H}_2\text{O}$, followed by 0.10 g of methylene blue under stirring. After 15 minutes, add 3.44 mL TEOS and stir for 4 hours. Silica-MB precipitation was taken by centrifugation and repeated washing with ethanol. A colloidal silica-methylene blue solution was prepared in 20 mL of water. Next, the silica-methylene blue particles were taken by centrifugation of the colloid solution and dried at a 70°C for 24 hours. After that, the synthesis results were dispersed in deionized water.

2.3. Synthesis of GO- NH_2

The results obtained from the synthesis of GO using the Hummer method were then used to be functionalized with amines (X. Liu et al., 2018). Added 40 mL of ethylene glycol under ultrasonication (Rahman et al., 2023). Then, 1 mL of air ammonia was added (Vishwakarma et al., 2023). The dark brown solution was transferred to a Teflon-coated autoclave for a

solvothermal reaction at 180°C for 10 hours. After the reaction, filter, and repeated with deionized water, oven at 60°C for 24 hours. Then the synthesis results are dispersed in deionized water. Furthermore, Raman and FTIR characterization was carried out.

2.4. Synthesis of Silica-MB@GO-NH₂ Particle

The preparation of Silica-MB was performed based on the report of literature (Q. Yang et al., 2019). 2 mL of volume and GO-NH₂ prepared, which volume was 100 μL. Mix all of them by adding 200 μL of ammonia. Next, the mixture was centrifugated and washed with ethanol three times. After that, the mixture was dried in a vacuum chamber. The result was obtained and characterized by SEM and Raman spectroscopy.

2.5. Fabrication of Paper-Based Sensor

The preparation was conducted by mixing 20 ml of water with addition of 1g PVA-1788. Next, the mixture of silica-MB@GO-NH₂ was poured into it. Next, the mixture was dripped onto the cellulose paper and dried at room temperature for 30 minutes. The paper was cut into small pieces and stored in a sealed bag. It will be used for the preparation of detecting NaOCl in the environmental sample such as tap water and swimming pool water. Eventually, a paper-based sensor will be tested below the UV-A lamp to determine the color of luminescence.

3. Results and Discussion

3.1. Synthesis of Particle Silica-MB@GO-NH₂

Silica-MB@GO-NH₂ particles were synthesized by solid agitation of mixture and repeatability of centrifugation. The reaction mechanism stabilized methylene blue, which is covered by silica and can also stick GO-NH₂ to obtain oxidation by chloramine.

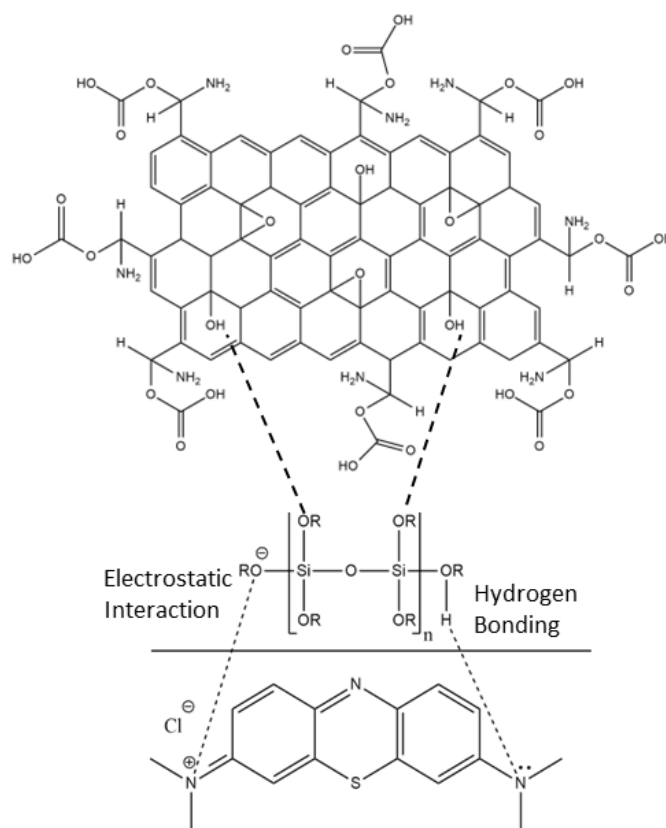


Figure 1. Mechanism of Silica-MB@GO-NH₂

First, the Hummers Methods was used in the fabrication of GO-NH₂ by mixing the GO material and 1 ml of ammonia 0.1 M in 40 ml ethylene glycol (98%).

Additionally, the addition of ethylene glycol as organic solvent was carried out on GO under ultrasonication to be modified by ammonia (GO-NH₂). Ethylene glycol (EG) was chosen because it could produce stable complexes with various functional groups especially with amine groups. This happens because ammonia can react with OH bond from carbonyl group through ethylene glycol bridging molecules. The probable reason is the carbonyl group has the lowest energy attraction compared to another functional groups. Furthermore, EG was used to avoid the interaction of ammonia with the carbonyl functional group. This mechanism is proposed to maintain unwanted compounds to inhibit the binding molecules and produce clear GO-NH₂. Moreover, the addition of ammonia to the GO is to functionalize graphene oxide into GO with amine groups. Following this, silica-MB and GO-NH₂ combine via hydrogen bonding to form a substrate called silica-MB@GO-NH₂.

In summary, FTIR was used to evaluate the functional group of prepared material. As seen figure 2a it showed chemical bond in silica-MB@GO-NH₂ particle using FTIR. Furthermore, the main source of silica particle fabrication uses the basic material TEOS, so it needs to be compared. The FTIR characterization discovered some peaks at the wavelength of 3457 cm⁻¹, 1611 cm⁻¹, 958 cm⁻¹, 1391 cm⁻¹, and 1079 cm⁻¹ accepted presence of stretching N-H, stretching C=C, bending O-H, and Si-O-Si bond which indicates the formation of silica-oxygen bonds in silica-MB commonly (H. Huang et al., 2020; Jain & Steel, 2015). Furthermore, the peak with a linear wavelength occurred at 1079 cm⁻¹ in all three compounds. This shows that the use of TEOS to make silica will not disappear completely. Then, there is a typical MB peak at 3457 cm⁻¹ which is still present in the substrate particles. Although the addition of the chloramine group did not reduce the MB completely in these particles. Briefly, this infrared peak showed that the formation of silica-MB and GO-NH₂ has been carried out successfully.

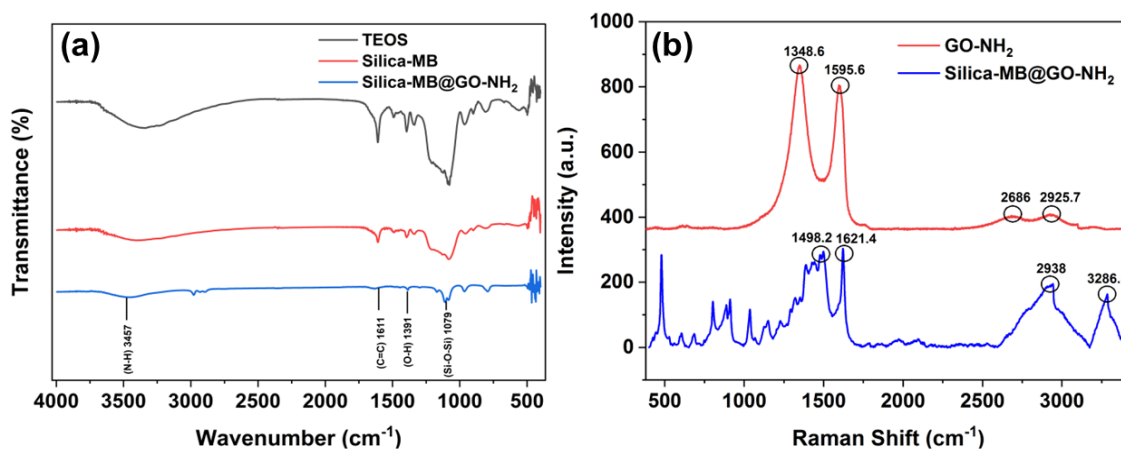


Figure 1. The measurement of (a) FTIR for TEOS, Silica-MB. And Silica-MB@GO-NH₂ and (b) Raman spectroscopy for GO-NH₂. And Silica-MB@GO-NH₂

As carbon base material, we conduct Raman spectroscopy to determine the GO material that is highly ordered in modification with NH₂. Figure 2b shows Raman spectrum of GO-NH₂ which has been obtained at the wavelength of 1595.62 cm⁻¹ and 1348.64 cm⁻¹ and silica-MB@GO-NH₂ at the wavelength of 1621.40 cm⁻¹ and 1498.27 cm⁻¹ which are related to G band and D band. The D band indicates a defect in graphitic structure rising from out of plane vibration while G band originate from in plane vibration of C-C bond from sp² orbital indicate graphite structure (Roslan et al., 2017).

Two samples displayed almost the same peak intensity ratio ID/IG = 1.08 for GO-NH₂ and ID/IG = 0.98 for silica-MB@GO-NH₂. On the other hand, the ratio between intensities of D and G band determines quality factor of carbon compound and graphene structure. The effect of hydrogen appears to increase quality of graphene structure where

the ID/IG ratio had been decreased from 1.09 to 0.98 (Das et al., 2007). The peak outside ID/IG is a typical peak of the methylene blue compound at wavenumbers of 495 cm^{-1} and 770 cm^{-1} . Meanwhile, there is a typical peak of silica, namely in the 1200 cm^{-1} (Ivanda et al., 2003; Li et al., 2016). This indicates that methylene blue and silica still exist in the material.

Silica-MB and Silica-MB@GO-NH₂ exhibited a spherical shape which was examined by electron microscope, respectively (Figure 3a and b). Moreover, the modification of silica particle with GO-NH₂ expose homogenous particle with average diameter 288 nm which carried out using ImageJ software. This result was larger than the pristine Silica-MB particle size at 253 nm. These phenomena proclaim that the modification of silica particle with the GO-NH₂ was successfully formed by increasing the particle size through methylene blue bridging bond.

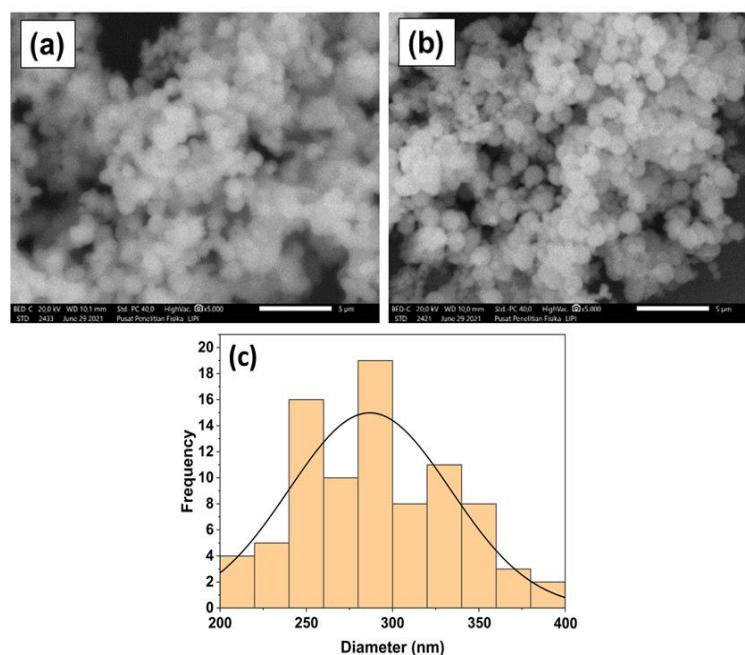
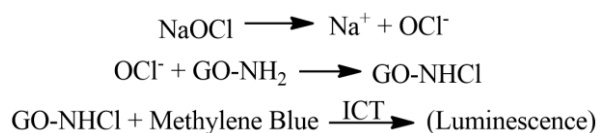


Figure 2. SEM Images of (a) Silica MB, (b) Silica-MB@GO-NH₂ at 5000x magnification and (c) Distribution of Silica-MB@GO-NH₂ particle

3.2. The Fluorescence Study of Silica-MB@GO-NH₂ as Paper-based Sensor

The preliminary fluorescence response was performed under UV-A lamp to determine the luminescence response of prepared material as paper-based sensor using $10\ \mu\text{L}$ NaOCl $90\ \mu\text{M}$ (optimal concentration).



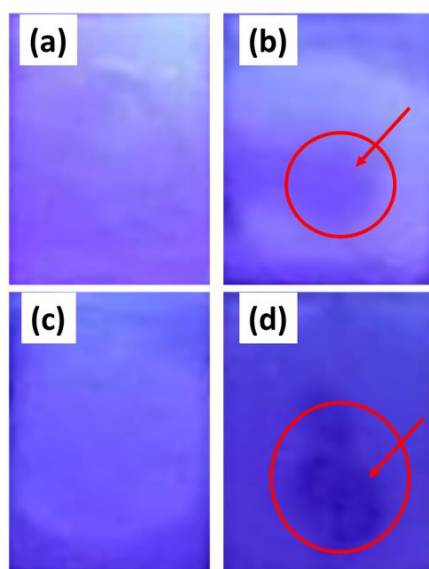


Figure 4. The fluorescence response on the UV-A lamp (a) before and (b) after dip 90 μM of NaOCl on the Paper blank immobilized by GO-NH₂ then (c) and (d) after dip 90 μM of NaOCl on the paper blank immobilized by silica-MB@GO-NH₂

In Figure 4, the paper-based sensor under UV Lamp A gives fluorescence response color from blue into dark purple at GO-NH₂ and dark blue in the presence of Silica-MB@GO-NH₂. In GO-NH₂, there is no significant difference in color changes after dripping NaOCl on paper blank. This is possible because the absence of MB as a fluorophore compound, which means there is no donor and acceptor electron transfer process that produces color emissions. The phenomenon is happening due to the complementary color wheel, blue is shown at a wavelength of 430-495 nm. Then, the resulting is the opposite color from blue with a wavelength of 485-620 nm (Algar et al., 2016). In summary, NaOCl existed on the surface of substrate which reacted with the luminophore MB followed by the radical's attraction. Briefly, the color luminescence results obtained explained that the paper-based sensor could work well.

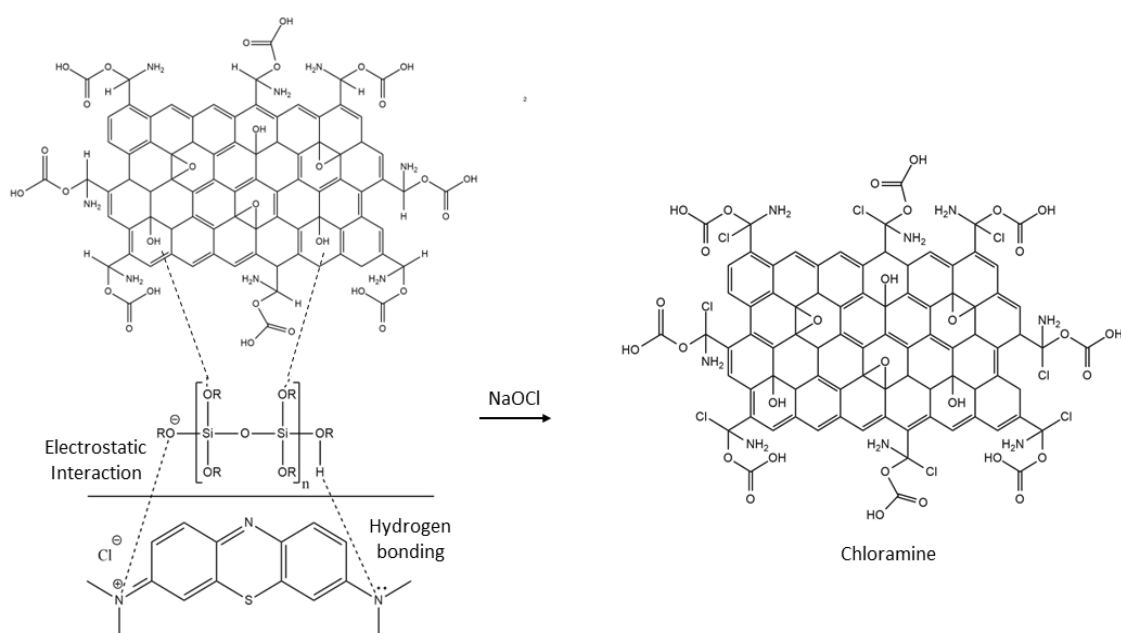


Figure 5. Mechanism of silica-MB@GO-NH₂ after dipping with NaOCl

The mechanism of substrate after immobilizing with NaOCl is depicted in Figure 5. When the particles have formed, the NaOCl sample is dripped using paper-based media. The H bonds in GO-NH₂ will be replaced with Cl⁻ bonds originating from NaOCl with substitution reaction.

To perform the fluorescence study, a laser beam from UV-DRS (Ultraviolet-Diffuse Reflectance Spectroscopy) is used to excite the electrons in specific compounds molecules, causing them to release light. The purpose is to measure and identify the molecule attraction from the sample (F. Al-Rawashdeh, 2012). The electrons are excited from the ground state (low energy level) to the excited state (high energy level) follows the fluorescence pathways and relaxed back to the ground state by exiting a specific wavenumber (Bose, Thomas, & Abraham, 2018). The reflectance response was exhibited from the addition of 10 μ L NaOCl 90 μ M into the surface of substrate. Based on figure (6a), the paper-based sensor can absorb light in UV-DRS measurement. Furthermore, the result was clear that both samples have a curved, steep absorption edge in the visible range. It suggests that they share optical characteristics as well as after exposed NaOCl that makes decrease at a wavelength of 239 nm which correlated with the amount of concentration added to the surface. In summary, the resulting substrate absorbance can work under an ultraviolet (UV) system (100-400 nm).

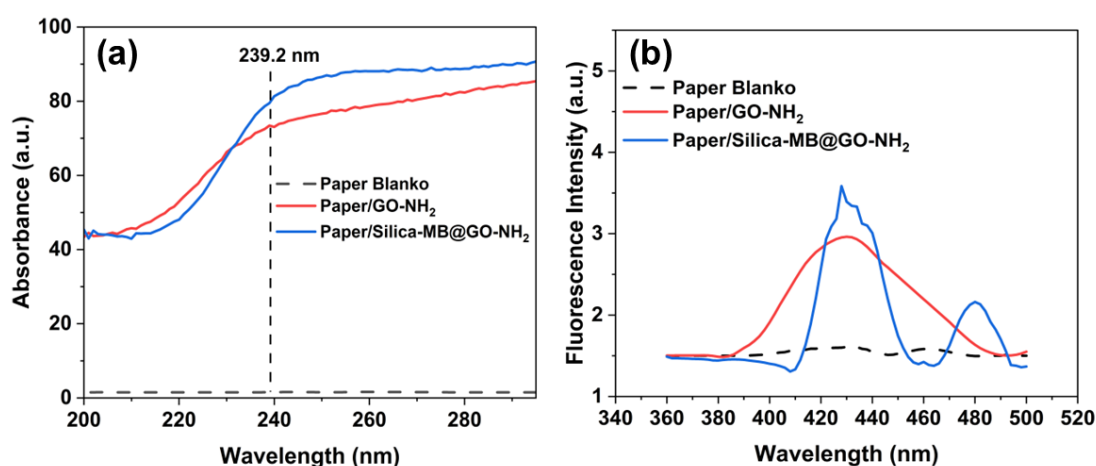


Figure 6. (a) UV-DRS spectroscopy and (b) Fluorescence spectroscopy of paper blank, paper with GO-NH₂ and paper with Silica-MB@GO-NH₂

The prepared material was examined using fluorescence spectroscopy to determine the performance of substrate for the NaOCl sensor application. In Figure 6b, the GO-NH₂ and Silica-MB@GO-NH₂ particles show dual emissive spectrum which belongs to Silica-MB particles (585nm) and GO-NH₂ nanosheets (427nm), respectively. Nevertheless, blank paper has no intensity because of the lack of substrate inserted that interacts with NaOCl so the chloramine process does not occur. On the other hand, depending on the fluorescence intensity of the NaOCl compound, NaOCl itself has its own function as an oxidizing agent and forms the OCl⁻ radical compound. To create a chloramine molecule, it will engage with the amino group GO-NH₂ through intramolecular charge-transfer (ICT) which initiates the dimming of fluorescence process (Misra & Bhattacharyya, 2018). The ICT process occurs excitation process who initiate by photon through molecules with a π -electron bridge between the donor and acceptor groups which generated by an absorption of light at specific wavelength (Pattison & Davies, 2006). This is where MB contributes to this process. So that, the resulting emission color will appear in the form of spectrum data. In short, the presence of the substrate on paper-based sensor will be important to give rise to higher fluorescence signal intensity upon NaOCl detection.

Figure 7 explains the fluorescence spectroscopy with NaOCl variation concentration. The result defined that without immobilization of substrate on paper-based sensor cannot produce fluorescence intensity. However, after adding GO-NH₂, the intensity

starts to increase because amine groups can oxidize to chloramine and then induce the quenching fluorescence supported by intramolecular transfer interactions. Furthermore, this may happen when higher quantities of fluorescent molecules, or fluorophores, tend to increase fluorescence intensity following Eq 1. On the other hand, using Silica-MB@GO-NH₂ was found to increase the intensity of fluorescence due to silica having stable photosensitivity properties (Mahović Poljaček et al., 2021). Moreover, there is a shift in the fluorescence peak that occurs as concentration increases. This may happen because of electron transfer quenching can occur when a quencher molecule accepts an electron from the excited-state fluorophore which can involve delocalized electrons in the fluorophore's excited state (Di et al., 2019). Although the fluorescence peak shifted with increasing NaOCl concentration, the results were linear between the higher concentration and the fluorescence intensity.

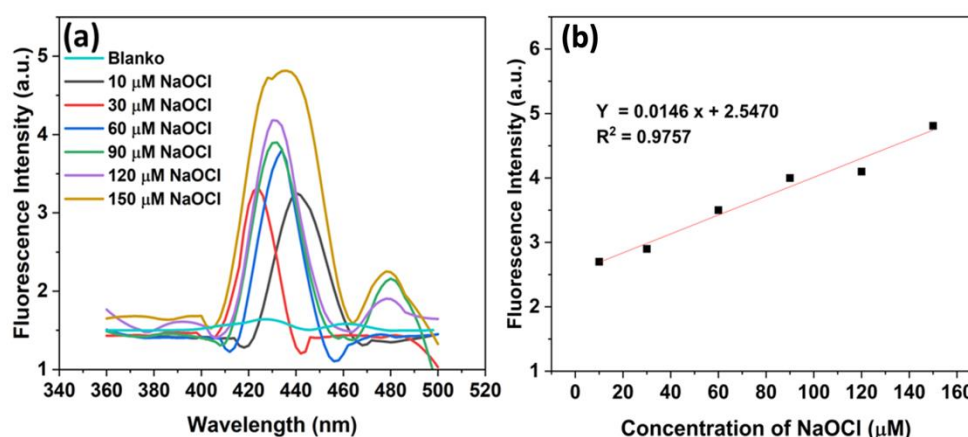


Figure 7. Fluorescence spectroscopy on the paper immobilized by Silica-MB@GO-NH₂ on (a) variation NaOCl concentration (b) linearity curve

In fluorescence spectroscopy, the intensity of emitted light (F) can be described with the equation below:

$$F = 2.303 \Phi I_0 abC \quad (1)$$

Where F the intensity of fluorescence, Φ is number of photons emitted, a is absorptivity, b is cuvette thickness and C is the concentration (M) of the fluorescent substance.

Moreover, the sensor performance was examined using NaOCl standard solution to determine the correlation between the increasing hypochlorite concentration with the fluorescence response/intensity. The graph 7.b explains the developing methods serve good linearity in the fluorescence measurements with regression value $R^2=0.9757$ and equation value $y=0.0146x + 2.54$. The ability of developed sensor to detect the analyte was dependent on the LOD and LOQ value. The LOD is lowest matching quantity to be deduced from the signal, which may be seen with a high enough level of confidence or statistical significance whereas the lowest concentration at which the analyte can be consistently identified and at which certain predetermined goals for bias and imprecision are reached is known as the limit of quantitation (LOQ) (Armbruster & Pry, 2008). The detection and quantification limit value were calculated by divide the standard deviation (S) with the slope from the linear equation, where the LOD and LOQ represented as $3S/b = 2.60 \mu\text{M}$ and $10S/b = 7.88 \mu\text{M}$, respectively.

Additionally, the performance comparisons with other method detection methods such as fluorescence, fluorescence quenching, and other electrochemical methods (μPAD), smartphone-based spectrophotometer are shown below in Table 1. Using diffuse reflectance techniques with particle of silica-MB@GO-NH₂ as the probe results in small value LOD were compared with other detection methods. Furthermore, these particles are supported by paper-based sensors or chitosan paper where the basic material is silica. Silica

has a good conductivity value so that it can produce phosphorescent colors with better percentage recovery results (Moyassari et al., 2022).

Table 1. Comparison of different reported methods for the detections of NaOCl

| Substrate | Method | LOD (μM) | LOQ (μM) | Sensitivity |
|--|--------------------------|-----------------------|-----------------------|--|
| CuO-NPs@MWCNT/epoxy [9] | Amperometry | 4.40 | 8.80 | -432.5 nA.L.mg ⁻¹ |
| N-CQDS [10] | Fluorescence Quenching | 0.43 | 1.04 | - |
| Benzothiazole [11] | Fluorescence | 11.26 | 43.50 | - |
| Luminol (Rahmawati et al., 2022b) | Electrochemiluminescence | 0.88 | 2.95 | 18.56 a.u. $\mu\text{M}^{-1} \text{cm}^{-1}$ |
| Silica-MB@GO-NH ₂ This work | Fluorescence | 2.60 | 7.88 | 1.2677 .L ⁻¹ |

3.3. Application of Silica-MB@GO-NH₂ as Paper-based Sensor for NaOCl Detection

To figure out the sensor performance, an application procedure was performed to determine NaOCl concentration in tap water and swimming pool water samples. The application process was conducted using 3 different methods like UV-A lamp, UV-DRS, and Fluorescence. Figure 8 shows that the concentration of NaOCl on the prepared substrate has been found higher on the swimming pool sample than in tap water. Moreover, the comparable method was completed by UV-DRS and fluorescence, where both methods result similar intensity trend (Figure 8.b-c) which expose more higher NaOCl concentration on swimming pool sample compared to the tap water sample. Additionally, to validate the sensor performance we have done measure the concentration of real sample with the addition of various concentration. Based on the calculations in Table 2, the developed sensor has good performance to determine the NaOCl concentration for tap water and swimming pool water for fluorescence spectroscopy and UV DRS spectroscopy with percent recovery sample range from 3.65 – 6.67 % and 0.05 – 0.14 % after calculated using each of its linearity equation, respectively.

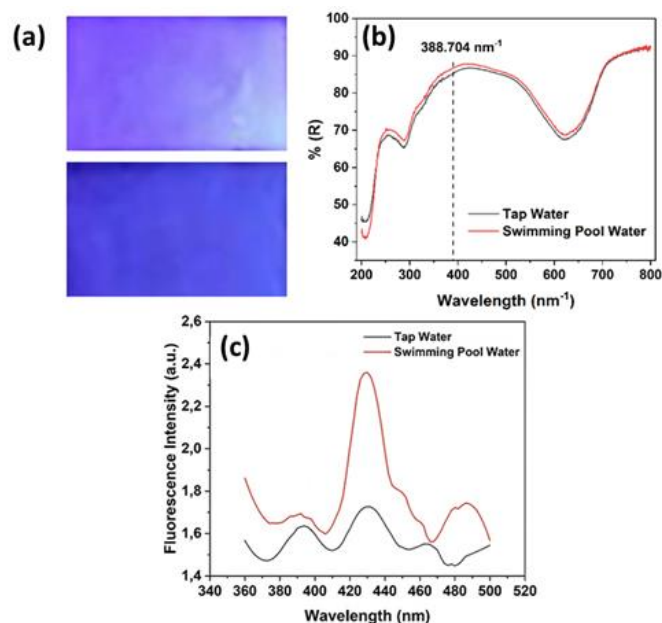


Figure 8. Application of Silica-MB@GO-NH₂ as paper-based sensor to detect NaOCl compound in (a) UV-A lamp with the tap water (red line) and the swimming pool (black line) with (b) results of %reflectance in UV DRS spectroscopy (c) fluorescence intensity using fluorescence spectroscopy

Table 2. Application of the prepared particle silica-MB@GO-NH₂ modified paper base sensor to detect NaOCl species in tap water and swimming pool water samples

| Methods | Water samples | Concentration (μM) | Detected | %Recovery |
|--------------|---------------------|--------------------|----------|-----------|
| UV- DRS | Tap Water | 10 | 9.54 | 95.44 |
| | | 20 | 20.91 | 104.00 |
| | | 30 | 29.54 | 98.46 |
| | Swimming pool water | 10 | 9.14 | 91.40 |
| | | 20 | 21.71 | 108.00 |
| | | 30 | 29.14 | 97.13 |
| Fluorescence | Tap Water | 10 | 11.09 | 110.90 |
| | | 20 | 17.86 | 89.30 |
| | | 30 | 31.09 | 103.60 |
| | Swimming pool water | 10 | 10.37 | 103.70 |
| | | 20 | 19.24 | 96.20 |
| | | 30 | 30.82 | 102.70 |

4. Conclusions

Silica-MB@GO-NH₂ particle effectively synthesized by mixing Stober's and Hummer's method with the result size of 288 nm and have spherically formed with aggregation formation. In fluorescence measurement, the intensity of fluorescence after using substrate increases more than using GO-NH₂ due to silica having stable photosensitivity properties and with supporting of MB can resulting emission color in the form of spectrum data. Moreover, the higher concentration can increase the intensity of fluorescence measurement because of the self-quenching from chloramine via intra-molecular charge transfer (ICT). UV-DRS demonstrated outstanding performance in the detection of NaOCl with a recovery percentage ranging from 91.40% to 108.00%. Additionally, 57.97 and 17.5 μM respectively, were calculated as the limits of detection and quantification from fluorescence measurement. Furthermore, the constructed sensor appears to be to be applied in practical usage due to its outstanding selectivity in the presence of some interference. At paper-based sensor, the colors appear pink colors as complementary color. Even though UV-A lamps are used in which the color does not display colors more clearly (which should be blue navy colors).

Acknowledgement

The authors acknowledge the financial support from Ministry of Education, Culture, Research and Technology, Republic of Indonesia via Directorate of Research and Development, Universitas Indonesia through Hibah PDD 2021 with contract number NKB-318/UN2.RST/HKP.05.00/2021.

Author Contribution

FRAAF: Conceptualization, data curation, formal analysis, and writing the original draft. IR and ARS: Analysis, validation, writing – review and editing. FRAAF and ARS: Data curation and formal analysis. ARS and JG: validation, funding acquisition, and supervisor.

Informed Consent Statement

Informed consent was obtained from all subjects involved in the study.

Conflicts of Interest

The authors declare no conflict of interest.

References

- Algar, W. R., De Jong, C. A. G., Maxwell, E. J., & Atkins, C. G. (2016). Demonstration of the Spectrophotometric Complementary Color Wheel Using LEDs and Indicator Dyes. *Journal of Chemical Education*, 93(1), 162–165. <https://doi.org/10.1021/acs.jchemed.5b00665>
- Armbruster, D. A., & Pry, T. (2008). Limit of Blank, Limit of Detection and Limit of Quantitation. In *Clin Biochem Rev* (Vol. 29). <https://www.ncbi.nlm.nih.gov/pmc/articles/PMC2556583/>
- Baek, Y., Kim, J., Ahn, J., Jo, I., Hong, S., Ryu, S., & Ha, N. C. (2020). Structure and function of the hypochlorous acid-induced flavoprotein RclA from *Escherichia coli*. *Journal of Biological Chemistry*, 295(10), 3202–3212. <https://doi.org/10.1074/jbc.RA119.011530>
- Böger, R., Rohn, K., Kemper, N., & Schulz, J. (2020). Sodium hypochlorite treatment: The impact on bacteria and endotoxin concentrations in drinking water pipes of a pig nursery. *Agriculture (Switzerland)*, 10(3). <https://doi.org/10.3390/agriculture10030086>
- Bose, A., Thomas, I., & Abraham, E. (2018). International Journal of Advances in Pharmaceutical Analysis Fluorescence spectroscopy and its applications: A Review QR Code *Correspondence Info. *International Journal of Advances in Pharmaceutical Analysis*. <https://doi.org/10.7439/ijapa>
- Bose, A., Thomas, I., Kavitha, G., Abraham, E., & Bose, A. (2018). *International Journal of Advances in Pharmaceutical Analysis Fluorescence spectroscopy and its applications: A Review *Article History: 08(01)*, 1–8: <https://doi.org/10.7439/ijapa.v8i1.4578>
- Budner, O., Cwalinski, T., Skokowski, J., Marano, L., Resca, L., Cwalina, N., Kalinowski, L., Hoveling, R., Roviello, F., & Polom, K. (2022). Methylene Blue Near-Infrared Fluorescence Imaging in Breast Cancer Sentinel Node Biopsy. *Cancers*, 14(7). <https://doi.org/10.3390/cancers14071817>
- Carlsson, K., Moberg, L., & Karlberg, B. O. (1999). *The Miniaturisation of the Standard Method Based on the n, n' -diethyl- p -phenylenediamine (dpd) Reagent for the Determination of Free or Combined Chlorine*. 33(2). [https://doi.org/10.1016/S0043-1354\(98\)00203-6](https://doi.org/10.1016/S0043-1354(98)00203-6)
- Chung, I., Ryu, H., Yoon, S. Y., & Ha, J. C. (2022). Health effects of sodium hypochlorite: review of published case reports. In *Environmental Analysis Health and Toxicology* (Vol. 37, Issue 1). <https://doi.org/10.5620/eaht.2022006>
- Cwalinski, T., Polom, W., Marano, L., Roviello, G., D'angelo, A., Cwalina, N., Matuszewski, M., Roviello, F., Jaskiewicz, J., & Polom, K. (2020). Methylene blue—current knowledge, fluorescent properties, and its future use. In *Journal of Clinical Medicine* (Vol. 9, Issue 11, pp. 1–12). MDPI. <https://doi.org/10.3390/jcm9113538>
- Das, A., Chakraborty, B., & Sood, A. K. (2007). *Raman spectroscopy of graphene on different substrates and influence of defects*. <http://arxiv.org/abs/0710.4160>
- Di, Y., Cui, X., Liu, Y., Zhou, C., Ren, Y., Di, Y., & Yang, X. (2019). Crystal structure, optical properties, and antibacterial activity of rare earth complexes with designed 2-carbonyl propionic acid-4-nitro benzoyl hydrazone. *Polyhedron*, 171, 571–577. <https://doi.org/10.1016/j.poly.2019.07.036>
- Enderlein, J., Ruckstuhl, T., & Seeger, S. (1999). Highly efficient optical detection of surface-generated fluorescence. *Applied Optics*, 38(4), 724. <https://doi.org/10.1364/ao.38.000724>
- Endo, T., Yoshimura, T., & Esumi, K. (2004). Voltammetric study of sodium hypochlorite using dendrimer-stabilized gold nanoparticles. *Journal of Colloid and Interface Science*, 269(2), 364–369. [https://doi.org/10.1016/S0021-9797\(03\)00674-X](https://doi.org/10.1016/S0021-9797(03)00674-X)
- F. Al-Rawashdeh, N. A. (2012). Current Achievement and Future Potential of Fluorescence Spectroscopy. In *Macro to Nano Spectroscopy*. InTech. <https://doi.org/10.5772/48034>
- Goswami, S., Aich, K., Das, S., & Pakhira, B. (2015). A Triphenyl Amine-Based Solvatofluorochromic Dye for the Selective and Ratiometric Sensing of OCl⁻ in Human Blood Cells. 1–8. <https://doi.org/10.1002/asia.201403234>

- Greasley, S. L., Page, S. J., Sirovica, S., Chen, S., Martin, R. A., Riveiro, A., Hanna, J. V., Porter, A. E., & Jones, J. R. (2016). Controlling particle size in the Stöber process and incorporation of calcium. *Journal of Colloid and Interface Science*, 469, 213–223. <https://doi.org/10.1016/j.jcis.2016.01.065>
- Huang, H., Wang, Y., Zhang, Y., Niu, Z., & Li, X. (2020). Amino-functionalized graphene oxide for Cr(VI), Cu(II), Pb(II) and Cd(II) removal from industrial wastewater. *Open Chemistry*, 18(1), 97–107. <https://doi.org/10.1515/chem-2020-0009>
- Huang, X., Li, Z., Cao, T., Cai, Q., Zeng, C., Fu, H., & Hu, L. (2018). A methylene blue-based near-infrared fluorescent probe for rapid detection of hypochlorite in tap water and living cells. *RSC Advances*, 8(26), 14603–14608. <https://doi.org/10.1039/c8ra01037d>
- Ishmah, S. N., Permana, M. D., Firdaus, M. L., & Eddy, D. R. (2020). *Extraction of Silica from Bengkulu Beach Sand using Alkali Fusion Method*. 4(2), 1–5. <https://doi.org/10.33369/pendipa.4.2.1-5>
- Ivanda, M., Clasen, R., Hornfeck, M., & Kiefer, W. (2003). Raman spectroscopy on SiO₂ glasses sintered from nanosized particles. *Journal of Non-Crystalline Solids*, 322(1–3), 46–52. [https://doi.org/10.1016/S0022-3093\(03\)00172-8](https://doi.org/10.1016/S0022-3093(03)00172-8)
- Jain, R., & Steel, T. (2015). *Waterborne inorganic-organic hybrid coatings on magnesium by sol-gel route Submitted for the partial fulfillment of the requirements for the degree of Master of Technology by Rachna Jain Corrosion Science and Engineering Indian Institute of Technology Bom. July*. <https://doi.org/10.13140/RG.2.1.3457.1368>
- Li, C., Huang, Y., Lai, K., Rasco, B. A., & Fan, Y. (2016). Analysis of trace methylene blue in fish muscles using ultra-sensitive surface-enhanced Raman spectroscopy. *Food Control*, 65, 99–105. <https://doi.org/10.1016/j.foodcont.2016.01.017>
- Liu, J., Chen, S., Liu, Y., & Zhao, B. (2022). Progress in preparation, characterization, surface functional modification of graphene oxide: A review. In *Journal of Saudi Chemical Society* (Vol. 26, Issue 6). Elsevier B.V. <https://doi.org/10.1016/j.jscs.2022.101560>
- Liu, X., Ma, R., Wang, X., Ma, Y., Yang, Y., Zhuang, L., Zhang, S., Jehan, R., Chen, J., & Wang, X. (2019). Graphene oxide-based materials for efficient removal of heavy metal ions from aqueous solution: A review. In *Environmental Pollution* (Vol. 252, pp. 62–73). Elsevier Ltd. <https://doi.org/10.1016/j.envpol.2019.05.050>
- Liu, X., Shi, L., Jiang, W., Zhang, J., & Huang, L. (2018). Taking full advantage of KMnO₄ in simplified Hummer's method: A green and one pot process for the fabrication of alpha MnO₂ nanorods on graphene oxide. *Chemical Engineering Science*, 192, 414–421. <https://doi.org/10.1016/j.ces.2018.07.044>
- Mahović Poljaček, S., Tomašegović, T., Leskovšek, M., & Stanković Elesini, U. (2021). Effect of SiO₂ and TiO₂ nanoparticles on the performance of uv visible fluorescent coatings. *Coatings*, 11(8). <https://doi.org/10.3390/coatings11080928>
- Misra, R., & Bhattacharyya, S. P. (2018). Intramolecular Charge Transfer. In *Intramolecular Charge Transfer*. Wiley-VCH Verlag GmbH & Co. KGaA. <https://doi.org/10.1002/9783527801916>
- Moyassari, E., Roth, T., Kücher, S., Chang, C.-C., Hou, S.-C., Spingler, F. B., & Jossen, A. (2022). The Role of Silicon in Silicon-Graphite Composite Electrodes Regarding Specific Capacity, Cycle Stability, and Expansion. *Journal of The Electrochemical Society*, 169(1), 010504. <https://doi.org/10.1149/1945-7111/ac4545>
- Pattison, D. I., & Davies, M. J. (2006). Evidence for rapid inter- and intramolecular chlorine transfer reactions of histamine and carnosine chloramines: Implications for the prevention of hypochlorous-acid-mediated damage. *Biochemistry*, 45(26), 8152–8162. <https://doi.org/10.1021/bi060348s>
- Rahman, M. O., Nor, N. B. M., Sawaran Singh, N. S., Sikiru, S., Dennis, J. O., Shukur, M. F. bin A., Junaid, M., Abro, G. E. M., Siddiqui, M. A., & Al-Amin, M. (2023). One-Step Solvothermal Synthesis by Ethylene Glycol to Produce N-rGO for Supercapacitor Applications. *Nanomaterials*, 13(4). <https://doi.org/10.3390/nano13040666>
- Rahmawati, I., Saepudin, E., Fiorani, A., Einaga, Y., & Ivandini, T. A. (2022a). Electrogenerated chemiluminescence of luminol at a boron-doped diamond electrode for the detection of hypochlorite. *Analyst*, 147(12), 2696–2702. <https://doi.org/10.1039/d2an00540a>

- Rahmawati, I., Saepudin, E., Fiorani, A., Einaga, Y., & Ivandini, T. A. (2022b). Electrogenenerated chemiluminescence of luminol at a boron-doped diamond electrode for the detection of hypochlorite. *Analyst*, 147(12), 2696–2702. <https://doi.org/10.1039/d2an00540a>
- Roslan, M. S., Chaudary, K. T., Haider, Z., Zin, A. F. M., & Ali, J. (2017). Effect of magnetic field on carbon nanotubes and graphene structure synthesized at low pressure via arc discharge process. *AIP Conference Proceedings*, 1824. <https://doi.org/10.1063/1.4978843>
- Sanjaya, A. R., Riyanto, H. G., Rahmawati, I., Putri, Y. M. T. A., Nurhalimah, D., Saepudin, E., Tesla, Y., & Krisnandi, Y. K. (2023). *EAM Environmental and Materials EAM 1(1): 28-40 Carbon-coated nickel foam for hypochlorous acid sensor*. 1(1). <https://doi.org/10.61511/eam>
- Shahzad, A., Köhler, G., Knapp, M., Gaubitzer, E., Puchinger, M., & Edetsberger, M. (2009). Emerging applications of fluorescence spectroscopy in the medical microbiology field. In *Journal of Translational Medicine* (Vol. 7). <https://doi.org/10.1186/1479-5876-7-99>
- Sharma, J., Sharma, S., Bhatt, U., & Soni, V. (2022). Toxic effects of Rhodamine B on antioxidant system and photosynthesis of *Hydrilla verticillata*. *Journal of Hazardous Materials Letters*, 3. <https://doi.org/10.1016/j.hazl.2022.100069>
- Smith, A. T., Marie, A., Zeng, S., Liu, B., & Sun, L. (2019). Nano Materials Science Synthesis, properties, and applications of graphene oxide / reduced graphene oxide and their nanocomposites. *Nano Materials Science*, 1(1), 31–47. <https://doi.org/10.1016/j.nanoms.2019.02.004>
- Thiagarajan, S., Wu, Z., & Chen, S. (2011). Amperometric determination of sodium hypochlorite at poly MnTAPP-nano Au film modified electrode. *Journal of Electroanalytical Chemistry*, 661(2), 322–328. <https://doi.org/10.1016/j.jelechem.2011.08.009>
- Vishwakarma, R. K., Narayanam, P. K., Umamaheswari, R., & Polaki, S. R. (2023). Amino-functionalized graphene oxide membranes for efficient separation of Sr²⁺ ions. *Journal of Water Process Engineering*, 51(October 2022), 103329. <https://doi.org/10.1016/j.jwpe.2022.103329>
- Wang, Y., Yang, L., Liu, B., Yu, S., & Jiang, C. (2018). A colorimetric paper sensor for visual detection of mercury ions constructed with dual-emission carbon dots. *New Journal of Chemistry*, 42(19), 15671–15677. <https://doi.org/10.1039/C8NJ03683G>
- Wang, Z., Mei, L., Yang, X., Jiang, T., Sun, T., Su, Y., Wu, Y., & Ji, Y. (2023). Near-infrared fluorophores methylene blue for targeted imaging of the stomach in intraoperative navigation. *Frontiers in Bioengineering and Biotechnology*, 11. <https://doi.org/10.3389/fbioe.2023.1172073>
- Yang, C., Feng, W., Li, Y., Tian, X., Zhou, Z., Lu, L., & Nie, Y. (2019). Graphene oxide based ratiometric fluorescent paper sensor for hypochlorous acid visual detection. *Journal of Photochemistry and Photobiology A: Chemistry*, 375, 141–147. <https://doi.org/10.1016/j.jphotochem.2019.02.021>
- Yang, Q., Zhang, C., Irvani, S., & Varma, R. S. (2019). *Green synthesis of Co₃O₄ nanoparticles using Euphorbia heterophylla L. leaves extract: characterization and photocatalytic activity* *Green synthesis of Co₃O₄ nanoparticles using Euphorbia heterophylla L. leaves extract: characterization and photo*. <https://doi.org/10.1088/1757-899X/509/1/012105>
- Yang, W., Zhang, C. G., Qu, H. Y., Yang, H. H., & Xu, J. G. (2004). Novel fluorescent silica nanoparticle probe for ultrasensitive immunoassays. *Analytica Chimica Acta*, 503(2), 163–169. <https://doi.org/10.1016/j.aca.2003.10.045>
- Yao, Z., Coatsworth, P., Shi, X., Zhi, J., Hu, L., Yan, R., Güder, F., & Yu, H. D. (2022). Paper-based sensors for diagnostics, human activity monitoring, food safety and environmental detection. In *Sensors and Diagnostics* (Vol. 1, Issue 3, pp. 312–342). Royal Society of Chemistry. <https://doi.org/10.1039/d2sd00017b>